

Article

Pre-Hatching Ontogenetic Changes of Morphological Characters of Small-Spotted Catshark (*Scyliorhinus canicula*)

Bianka Grunow ^{1,*}, Theresa Reismann ^{1,†} and Timo Moritz ^{2,3}

¹ Research Institute for Farm Animal Biology (FBN), Institute of Muscle Biology, Wilhelm-Stahl-Allee 2, 18196 Dummerstorf, Germany; theresa.reismann@uni-rostock.de

² Deutsches Meeresmuseum, Katharinenberg 14–20, 18439 Stralsund, Germany; timo.moritz@meeresmuseum.de

³ Institute of Biological Sciences, University of Rostock, Albert-Einstein-Straße 3, 18059 Rostock, Germany

* Correspondence: grunow@fhn-dummerstorf.de

† These authors contributed equally to this work.

Abstract: The small-spotted catshark, *Scyliorhinus canicula*, provides an optimal model organism to include chondrichthyans in studies comparing morphology or physiology through vertebrate evolution. In particular, for investigations with ontogenetic aspects, there are only a limited number of alternative taxa. Therefore, a detailed staging system is a prerequisite to allowing comparison between different studies. This study supplements information on the latest stages of the established system by Ballard and colleagues in 1993 and complements the respective staging system by including the latest pre-hatching stages. During this phase, some significant ontogenetic shifts happen, e.g., reduction of external gill filament length and complete flattening of rostral angle until Size Class 6, change in the ratio of pre- to post-vent length, and establishment of body pigmentation in Size Classes 7 and 8. All these shifts finally transform the embryo into a hatchling prepared for living outside the eggshell. This study provides a framework allowing comparison of investigations on pre-hatchings of the small-spotted catshark.

Keywords: lesser-spotted dogfish; cartilaginous; shark; larvae development; ontogeny; PCA



Citation: Grunow, B.; Reismann, T.; Moritz, T. Pre-Hatching Ontogenetic Changes of Morphological Characters of Small-Spotted Catshark (*Scyliorhinus canicula*). *Fishes* **2022**, *7*, 100. <https://doi.org/10.3390/fishes7030100>

Received: 15 March 2022

Accepted: 17 April 2022

Published: 26 April 2022

Publisher's Note: MDPI stays neutral with regard to jurisdictional claims in published maps and institutional affiliations.



Copyright: © 2022 by the authors. Licensee MDPI, Basel, Switzerland. This article is an open access article distributed under the terms and conditions of the Creative Commons Attribution (CC BY) license (<https://creativecommons.org/licenses/by/4.0/>).

1. Introduction

In recent decades, the volume of research studies published on chondrichthyans has increased enormously [1]. The increasing number of publications referring to catsharks in recent years, e.g., 2000–2010: 243 publications; 2011–2021: 307 publications [1], indicate that the genus *Scyliorhinus* (Chondrichthyes: Carcharhiniformes: Scyliorhinidae) is becoming a popular study model. The reasons for this are manifold. Cartilaginous fish, i.e., sharks, rays, and chimaeras, are evolutionarily very important, as they represent the sister group of osteognathostomes, i.e., bone-bearing vertebrates containing more than 98% of all vertebrate species. Most cartilaginous fish, however, are not easily accessible for many research questions, as they can hardly be kept in captivity. In particular, providing developmental stages in high numbers by breeding species in aquaria is not possible for most chondrichthyans. However, small-spotted catsharks are an exception. Due to their size and lifestyle, they can be kept in captivity. Furthermore, their reproductive style by depositing eggs without a pronounced reproductive phase makes ontogenetic stages quite easily and continuously accessible and, overall, makes it an attractive laboratory animal. Therefore, in developmental biology, catsharks offer an important perspective and are used to acquire a better understanding of the origin and diversification of jawed vertebrates [2]. The range of research topics indicates how intensively the catshark is studied with regard to partly very specific anatomical or also physiological properties of various organ systems such as the heart [3], sensory organs and nervous system [4], muscles [5,6], and gastrointestinal

tract [7] or immune system [8,9]. Most of these studies aim to compare properties partly with other cartilaginous or bony fishes or in the context of general vertebrate evolution.

However, there are only a few morphological studies on *Scyliorhinus*, and information on external characteristics is often missing, especially in premature stages. For adult sharks, Soares and De Carvalho (2019) investigated the 16 *Scyliorhinus* species of the family Scyliorhinidae [10]. In this study, the external morphological characteristics, neurocranium, claspers, dermal denticles, and tooth morphology for classifying the phylogenetic differences between the species were investigated. They indicated that, in particular, the small-spotted catshark (*S. canicula*) can be distinguished easily from its congeners due to the unique characteristics in its naso-oral region [10].

The small-spotted catshark belongs to the group of shallow-water sharks [11] and exhibits a stable population [12]. Embryos of *S. canicula* develop in egg cases deposited by the females in shallow water and attached to macroalgae or sessile invertebrates via the posterior tendrils [13]. The embryonic development of *S. canicula* takes 5 to 11, usually 8 to 9, months, depending on the water temperature [11]. Different developmental stages of the embryos were classified by external features observed microscopically by Ballard et al. (1993) [14]. This classification is used as the standard for the age-betting of *S. canicula*. The present study aims to follow up on the studies by Ballard et al. (1993) [14] and Soares and De Carvalho (2019) [10] to provide further insights into the morphological changes during development to understand the evolutionary changes of the *Scyliorhinus* in more detail, as ontogenetic changes in the external morphology provide valuable information for evolutionary questions. Additionally, the relationships between growth and morphological changes are relevant because they have an impact on the phenotypic diversity within species [15]. Therefore, the aim of this study is to present new insights into the developmental changes of external morphological traits during the pre-hatching phase (as defined by Ballard (1993) [14]). In particular, the development of the gill filament and rostrum angle, as well as the post- and pre-vent length, will help to better understand the origins of the peculiar appearance of the small-spotted catshark.

2. Materials and Methods

2.1. Morphometry

Embryos of small-spotted catsharks, *S. canicula*, were obtained from a collection of formol-fixed specimens stored in 70% ethanol, which were provided by Ozeaneum (Stralsund, Germany). Formal fixation was chosen, as it has been shown that this fixative has a neglectable influence on tissue shrinkage in catsharks [16]. All animals used in this study originated from 5 females and 4 males. Adult animals, as well as their eggs, deposited on plants, were kept in a 5000 L recirculating system with two separate divisions. In order to avoid differences in development due to changing abiotic parameters, the parameters were kept permanently constant: temperature of 14–15 °C, salinity of 2.5 PSU, and oxygen supply of 98.5%. Before fixation, all embryos were anesthetized using benzocaine solution (ethyl p-amino-benzoate; Sigma Aldrich; Taufkirchen, Germany) dissolved in aquarium water and euthanized with overdoses. Images of specimens were taken using a Canon EOS 80D camera system with a Canon MP-E 65 mm and Sigma DG Macro 105 mm objective mounted on a Cognisys StackShot unit. For Z-stacking, Helicon Focus (HeliconSoft, Kharkiv, Ukraine) software was used.

To gain insight into morphometric changes across different developmental stages, 107 specimens were photographed dorsally, laterally, and ventrally using a stereomicroscope (Leica SD9) combined with Motacam 5.0 (Motic; Carl Roth GmbH & Co. KG; Karlsruhe, Germany). Depending on the respective developmental stage, 15–19 morphometric parameters were analyzed for each individual utilizing Motic Images Plus (Version 3.0; Carl Roth GmbH & Co. KG; Karlsruhe, Germany) software. The selection of morphometric parameters was based on the work of Ballard et al. (1993) [14], Soares et al. (2016) [17], and Franz et al. (2021) [18]. For an additional, better understanding, the determined morphometric parameters are shown in Figure 1 and Table 1. For individuals that were

too large to fit under the stereomicroscope, total length (TL), pre-vent length (PRV), and post-vent length (POV) were measured employing digital calipers to the nearest 0.1 mm. Subsequently, eight size classes for the embryos were introduced, taking into account the staging system implemented by Ballard et al. (1993) [14], to gain a more detailed view of the pre-hatching period (Table 2, Figure 2).

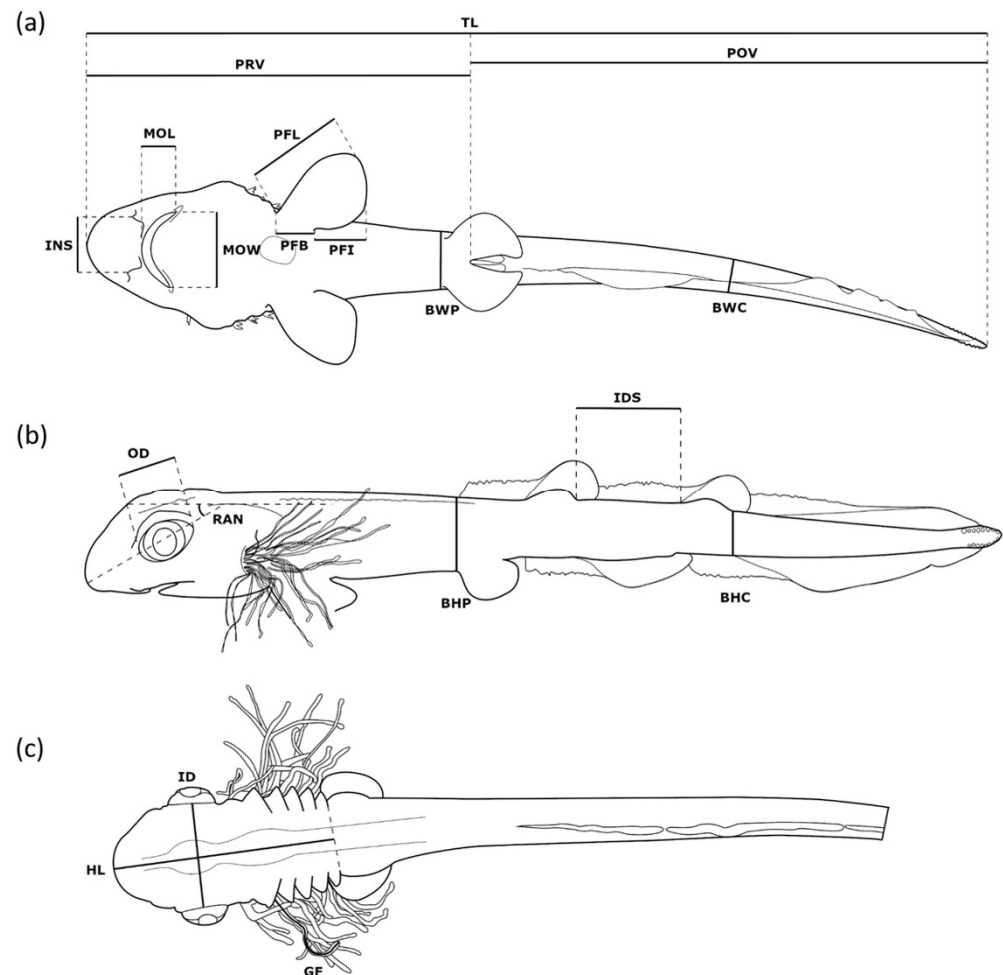


Figure 1. Position of measurements taken on developmental stages of *Scyliorhinus canicula*. (a) Measurements taken from ventral side: BWC—body width at caudal peduncle, BWP—body width at pelvic fin, INS—internostril space, MOL—mouth length, MOW—mouth width, PFB—pectoral fin base width, PFI—pectoral fin inner margin, PFL—pectoral fin length, POV—post-vent length, PRV—pre-vent length, TL—total length; (b) lateral side: BHC—body height at caudal peduncle, BHP—body height at pelvic fin, IDS—interdorsal space, OD—orbital diameter, RAN—rostrum angle; (c) dorsal side: GF—external gill filament length, HL—head length, ID—interorbital distance.

Table 1. Morphological parameters with their used abbreviations and description.

Abbreviation	Name	Description
BHC	Body depth at caudal peduncle	Maximal distance dorsal to ventral margin at base of caudal fin ¹
BHP	Body depth at pelvic fin	Maximal distance dorsal to ventral at origin of pelvic-fin base ¹
BWC	Body width at caudal peduncle	Maximal width at caudal peduncle
BWP	Body width at pelvic fin	Maximal width at origin of pelvic-fin base
GF	Gill filament length	Estimated average length of external gill filaments of second gill slit
HL	Head length	Distance from rostral tip to fifth gill slit
ID	Interorbital distance	Width of neurocranium between midlevel of eyes
IDS	Interdorsal space	Distance from first dorsal-fin base to second dorsal-fin base
INS	Internostril space	Distance between nostrils at base of anterior nasal flaps ²
MOL	Mouth length	Distance from anteriormost point of mouth opening to posterior level of cleft end along body axis
MOW	Mouth width	Distance from left to right corner of mouth
OD	Orbita diameter	Length of eye along body axis
PFB	Pectoral fin base	Width of pectoral-fin base
PFI	Pectoral fin inner margin	Length of posterior margin of pectoral fin
PFL	Pectoral fin length	Longest distance from anterior base to tip of pectoral fin
POV	Post-vent length	Body length from vent to end of tail
PRV	Pre-vent length	Body length from rostral tip to vent
RAN	Rostrum angle	Angle from rostral tip to body axis going anterior. Body axis is drawn from most distal anterior point over midpoint of otic capsule to midpoint of chorda at height of pectoral fin.
TL	Total length	Distance from rostral tip to end of tail

¹ Measuring only myomer height in early stages without fin fold; ² in early stages distance between nasal openings.

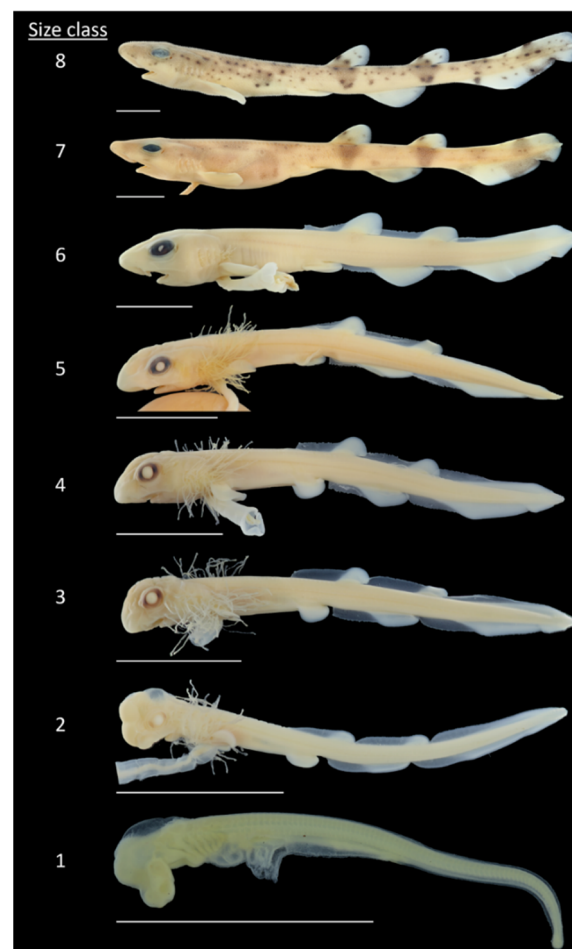


Figure 2. Small-spotted catshark (*Scyliorhinus canicula*). Embryos at different developmental stages and size classes from early development (Size Class 1) to late embryonic stage (Size Class 8) shortly before hatching. Scale 1 cm.

Table 2. Overview of examined developmental stages and size classes of *Scyliorhinus canicula*.

Size Class	n	Total Length (mm)	Stages According to Ballard et al. (1993)
1	11	9.7–16.8	24–26
2	13	18.0–27.0	27
3	16	28.6–33.8	28–29
4	14	35.2–44.8	31
5	14	46.7–59.6	32
6	9	61.1–69.9	34
7	10	77.5–87.7	Not defined
8	20	88.9–104.9	Not defined

Size Class 1. External gill filaments rarely present on C1 and C6. Pre-vent length greater than post-vent length.

Size Class 2. Anlagen of dorsal and anal fins appear in larval fin fold. Pre-vent and post-vent length about equal. First pigments appear in eyes.

Size Class 3. Complete circle of pigments on eyes. Pre-vent length smaller than post-vent length. Length of gill filaments more than half of head length. Mouth shape is curved.

Size Class 4. Embryonic placoid scales appear first on caudal tip and later in two rows along dorsal side. Anlagen of dorsal fins surmount fin fold.

Size Class 5. Length of gill filaments less than a third of head length. First pigment spots on flanks.

Size Class 6. Length of gill filaments less than or equal to a tenth of head length. Dorsal and anal fins twice as high as fin fold

Size Class 7. Complete leveling of rostrum angle. Dark bands below dorsal fins and on caudal fin appear. Fin fold completely reduced. Belly swollen due to internal yolk.

Size Class 8. First regular placoid scales emerge. Remnant of external yolk sac as small appendage.

2.2. Statistics

Analysis of the morphometric data was performed using GraphPad Prism 9. Size-class-grouped data were tested for normality, the Shapiro–Wilk test was conducted, and outliers were identified using the ROUT method ($Q = 1\%$) and excluded from further analysis. Differences between size classes were tested using ordinary one-way ANOVA, followed by Tukey’s multiple comparison post hoc test ($p < 0.05$). To allow for size-independent comparison, the measured values were normalized by converting them to a percentage of TL and reanalyzed.

Furthermore, a principal component analysis (PCA) was applied to reduce the dimensions of the morphometric data set to a smaller number of components, still containing most of the original information. The PCA was conducted using the original data, to examine if trait variation across the size classes supports this size-dependent staging system. Since PCA depends on the scaling of variables, data were normalized by setting the mean of each feature to 0 and the standard deviation to 1. PCA was performed using the Python package scikit-learn [19], and plots were generated with the Python package Matplotlib [20] and Seaborn [21].

For this comparison, the mean \pm S.E.M. were calculated, and differences between morphological parameters were tested using ordinary one-way ANOVA, followed by Tukey’s multiple comparison post hoc test (* $p < 0.05$).

3. Results

3.1. Morphometric Analysis

To gain an overview of the relationship between the individual morphometric characters determined in this study, a correlation analysis was performed (Figure 3a). In S.

canicula ontogeny, all analyzed morphometric parameters, except external gill filament length (GF) and rostrum angle (RAN), were highly positively correlated to each other, with a Pearson correlation coefficient greater than 0.9. GF showed no correlation, with a Pearson correlation factor of -0.3 . RAN was highly negatively correlated to all other morphometric features, with a mean Pearson correlation factor of -0.7 .

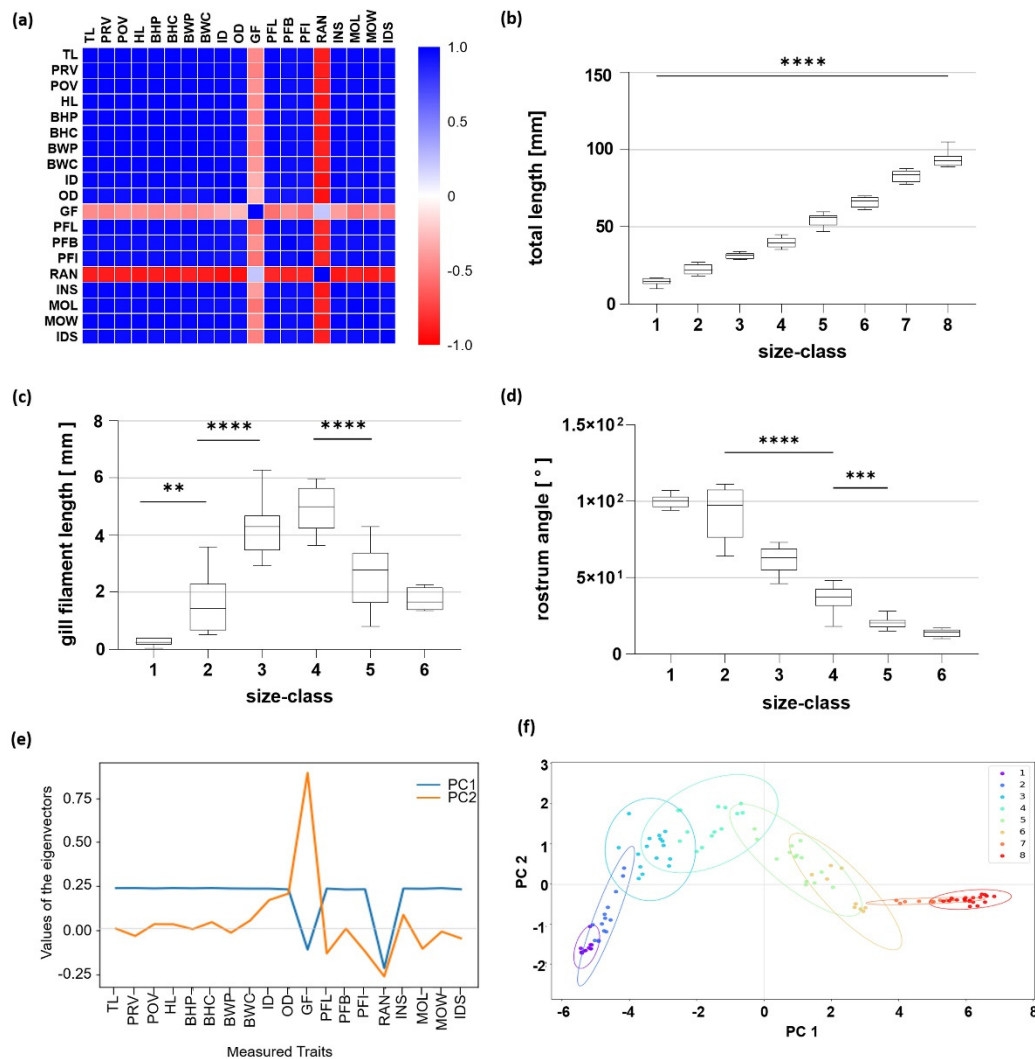


Figure 3. Analysis of morphometric features. (a) Correlation matrix of the obtained body parameters. The values for the Pearson correlation coefficient are color coded. (b–d) Changes in selected body parameters of *Scyliorhinus canicula* with increasing size classes from total length (b), gill filament (c), and rostrum angle (d). Significant changes are indicated by ** $p < 0.01$, *** $p < 0.005$, **** $p < 0.001$. (e,f) Results of the principal component analysis. (e) Values of the eigenvectors for the first two principal components (PCs). Contribution of the parameters to each PC is shown by the value of the eigenvector. (f) Plot of the first two PCs. Results are shown for each size class (color coded).

The TL of all observed specimens ranged from 9.7 to 104.9 mm, with a mean of 14.4 ± 0.7 mm and 93.5 ± 1.0 mm for Size Classes 1 and 8, respectively (Figure 3b). All measured parameters were found to increase with increasing size class (Supplementary Materials Table S1), except for GF and RAN. The course of GF resembles a bell shape, peaking in Size Class 4 with 4.9 ± 2.1 mm and a significant decrease to Size Class 5 (Figure 3c). In Size Classes 7 and 8, external gill filaments were no longer present. RAN considerably decreased from $92.1 \pm 4.6^\circ$ in Size Class 2 significantly to each further size class and exhibited an angle of around 20° in Size Class 5 and 13° in Size Class 6 (Figure 3d). Here, in Size Classes 7 and 8, the rostrum angle was no longer present.

The PCA analysis confirmed these data. PC1 and PC2 account for 96.9% of the total variation. The eigenvector of PC1 had a steady value of 0.25 for nearly all parameters. GF and RAN had the highest loading parameter in both PCs with a value of 0.87 and -0.25 , respectively (Figure 3e). In PC2, the main variables were markers of the head, such as OD, GF, RAN, INS, MOL, and IDS (Figure 3e). Within the PC plot, large deviations in Size Classes 2 to 6 for PC2 were visible, while hardly any differences could be detected in Size Class 1, as well as Size Classes 7 and 8. In addition, a transition point in Size Class 4 was present (Figure 3f).

3.2. Measurements in Relation to Total Length

In fish developmental research, an analysis of morphometric parameters in relation to fish length is important to detect changes in realities. In *S. canicula*, a considerable change in morphometric relationships was detected, as shown in the correlation matrix (Figure 4a, Supplementary Materials Table S2) compared to Figure 3a. Calculations in relation to the TL, the pre-vent length (PRV), and post-vent length (POV) are highly negatively correlated to each other. Moreover, GF and RAN no longer correlate negatively with each factor. There are also positive correlations, such as PRV, HL, and MOL.

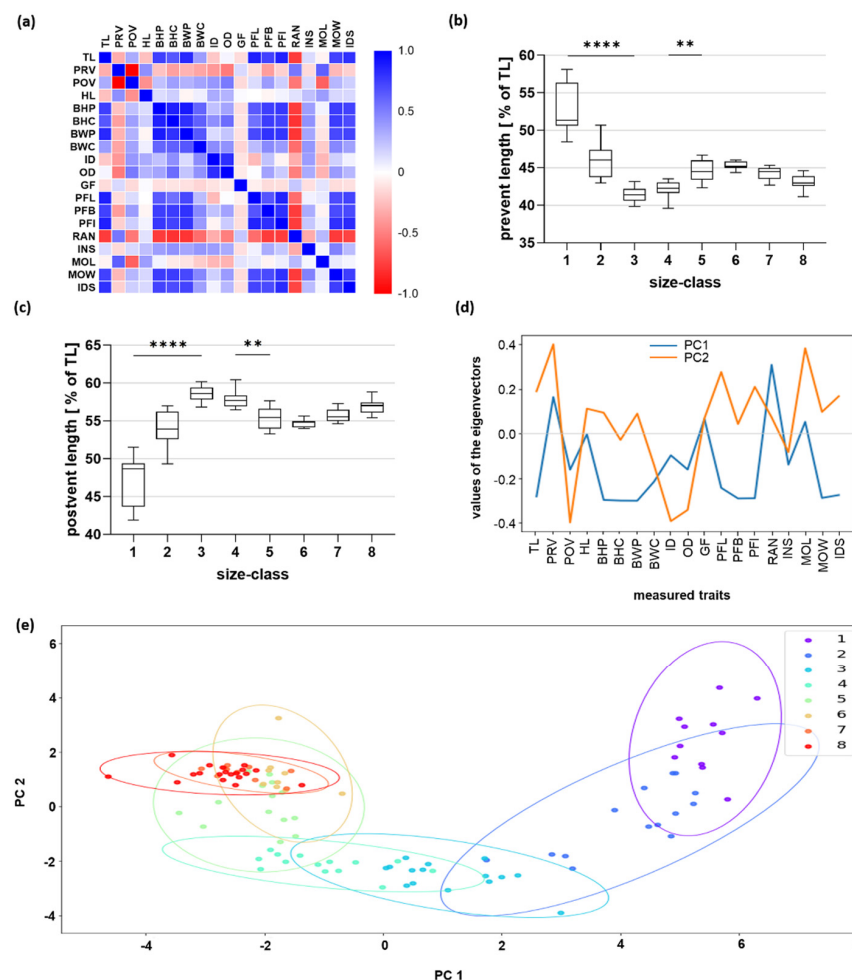


Figure 4. Analysis of morphometric features in relation to total length. (a) Correlation matrix of the obtained body parameters. The values for the Pearson correlation coefficient are color coded. (b,c) Changes in pre-vent length (b) and post-vent length (c) calculated in relation to TL of *Scyliorhinus canicula* with increasing size classes. Significant changes are indicated by ** $p < 0.01$, **** $p < 0.001$. (d,e) Results of the principal component analysis. (d) Values of the eigenvectors for the first two principal components (PCs). Contribution of the parameters to each PC is shown by the value of the eigenvector. (e) Plot of the first two PCs. Results are shown for each size class (color coded).

A shift in the ratios of PRV and POV despite bilateral growth in each age group is present (Figure 4b,c). In PRV, after a significant decrease between the first three size classes from $52.6 \pm 1.0\%$, in Size Class 1 down to $41.4 \pm 0.3\%$ until Size Class 3, PRV was nearly stable, except for a significant increase between Size Classes 4 and 5 (Figure 4b). Compared to PRV, POV displayed a reversed course. Here, a significant increase between the first three size classes (Size Class 1: $47.4 \pm 1.0\%$; Size Class 2: $54.3 \pm 0.6\%$; Size Class 3: $58.6 \pm 0.3\%$) and a significant decrease between Size Classes 4 and 5 were present (Figure 4c).

The PCA showed that for the calculated characteristics in relation to total length, PC1 and PC2 accounted for 63.0% of the total variation. In both PCs, it is visible that several measurement traits had an influence on the PCA. In PC1, besides the parameter RAN (loading parameter of >0.5), the parameters of the pectoral fin, such as PFL, PFB, and PFI, as well as of the body (BHP, BHC, BWP), are the main variables. PC2 is mainly loaded by PRV and mouth length (MOL), both ~ 0.4 , followed by POV and ID, with ~ -0.4 for both (Figure 4d). The distribution along PC2 shows that for progressing developmental stages, their values decline. The early stages are also more spread apart in their variation, while the later stages vary far less (Figure 4e).

4. Discussion

The traits selected for the definition of developmental stages follow the definitions of morphologically based landmarks rather than a time- or length-based system. This is due to the different gestation periods of different elasmobranch species [14,22–24] and, of course, depending on the water temperature during development. The development of the fish follows Vant Hoff's rule, i.e., within the tolerance range, the development is also faster with increasing temperature. However, it has already been shown that the hatching of catsharks takes place earlier at increased temperatures due to faster development, but the animals have a shorter length [25]. Therefore, in order to investigate the morphometric characteristics, this study focused on uniform abiotic parameters during breeding. Tanaka et al. (1990) described that the frilled shark (*Chlamydoselachus anguineus*) has perhaps the longest gestation period of up to 3.5 years [26], compared to the rather short period of usually 8 to 9 months in *S. canicula* [11]. Overall, the stages used in this study were well defined, and subsequent analyses reflected the grouping of individuals belonging to their respective stages.

4.1. Stages Leading to Pre-Hatching

The first stage examined here is comparable with Stages 24 to 26 defined by Ballard et al. (1993) [14]. During this stage, the first gill filaments appear, and the mouth opening becomes diamond shaped, which will remain so until Stage 27 [14]. The head is strongly inclined so that the rostrum angle is large. Somites are present up to the end of the tail.

In Size Class 2 (Stage 27 according to Ballard et al. 1993) [14], the gill filaments increase due to the eggshell opening and the resulting more active exchange with the environment. In some animals, the rostrum angle decreases, and the head straightens further, but due to the high variability between specimens, this was not significantly different from the stage before. At the same time, the post- and pre-vent length increases, but in relation to the TL changes. As the post-vent length increases in relation to the TL, the pre-vent length decreases. The reason for this can be manifold. It is possible more energy is needed for the further development of the inner organs because the eggshell is opened, and the metabolism must be rearranged. Therefore, the anterior body part grows less compared to the posterior body part. During this time, according to Ballard et al. (1993), the yolk sac is encased in an almost complete epithelial lining, half of which is underlain by a capillary network [14]. At this point, the catshark embryo is able to survive outside the eggshell. The greater length growth of the post-vent may also be caused by a more active embryo, as the muscle area in the post-vent part of the body increases. This increase in muscle mass is supported by the increase in body height in this part of the body. Only during the first

observed stage of the pre-hatching stages was no growth in the tail and pelvic parts of the body detectable.

In Size Class 3 (Stages 28 and 29 according to Ballard et al. 1993) [14], the mouth form changes from diamond to oval, and the pelvic fins obtain their rounded shape. A circle of black pigment becomes prominent in the eye. Shallow depressions in the low fin fold mark the posterior limits of the emerging two dorsal fins and the anal fin. While the individual morphometric length parameters continued to increase in size, the rostrum angle greatly reduced, and the head thus became more elongated.

4.2. Stages from Pre-Hatching to Hatching

The PCA indicated that the examined Size Class 4 (Stage 31 according to Ballard et al. 1993) [14] can be considered as the stage of portion shift. During this time, the PCA of the absolute measured values showed the maximum in PC2, while the parameters in relation to the TL showed a minimum of the PC2 values. Examining the individual parameters, the gill filaments reach their maximum length in Stage 4. Furthermore, the ratio of the post-vent length to the pre-vent length reaches its maximum.

In Size Classes 5 and 6 (Stages 32 and 34 according to Ballard et al. 1993) [14], the values of PC1 and PC2 indicate a strong change in the parameters. The causes include the external gill filaments, which decrease in length until they are fully degraded in Size Class 6 at a body length of about 65 mm, and pharyngeal respiration starts. The cat shark seems to be fully developed and resembles very much a miniature of an adult. Another reason for this strong change is the rostrum angle, which continues to flatten during this developmental step until the final position is reached. Additionally, the growth of the orbital diameter relative to the total length stops in Size Class 5 and reduces in Size Class 6.

As shown for bamboo shark (*Chiloscyllium punctatum*) [27], we described more details about the later stage than the catshark staging table by Ballard et al. (1993) [14] and added two further size classes to complete the developmental description until hatching.

In Size Class 7, the rostrum angle levels completely, and dark bands of pigmentation appear below the dorsal fins and on the caudal fin. The belly is swollen due to the internal yolk, and the larval fin fold is completely regressed.

In Size Class 8, the recession of the orbital diameter in relation to total length stops, and the first regular placoid scales emerge.

In these two classes, the catshark increases in body size, and all individual parameters increase in this context. Due to the increasing body size, the embryo becomes more immobile in the eggshell. The last stages are important because the longer the development takes place in the eggshell, the bigger the embryo can grow. The growth and hatching of the animal depend, among others, on the environmental temperature. *Scyliorhinus canicula* embryos used in this study were cultured at 15 °C. Embryos cultured at other temperatures show some heterochrony of developmental events, which is not surprising due to natural variation within a species. A study showed that the higher the water temperature, the smaller the hatchlings, which can be attributed to shorter developmental time and growth phase in the eggshell [25].

Additionally, during the last developmental stages, skin pigmentation becomes prominent. Both factors are important for survival, as the hunting pressure decreases with increasing body size, and pigmentation is important for camouflage. The patterning reduces the visibility of the animal against its background so that predators recognize their prey more poorly, and thus their survival in the early post-hatching stage is improved. In addition, the prey is also less able to recognize the danger. In catshark species, besides the individual pigmentation of the animals [28], sexual dimorphism in pigmentation is also present [17]. Additionally, adult females have thicker dermal layers compared to males due to male biting during mating [29]. The presence of sexual dimorphism has already been described by Ford (1921) [30]. This study indicated that these gender differences become established at 53 to 60 cm when reaching sexual maturity. For mouth length and width,

it was also shown that MOL/MOW significantly differed between sexes, but only in the larger size groups and not for specimens below 42.5 cm [31].

Sex-specific differences in morphological parameters are not very likely to be present at this early life stage but should be carefully investigated in further studies.

5. Conclusions

Shortly before hatching, embryos of *S. canicula* undergo morphological changes. These are visible by total flattening of the rostral angle and the establishment of body pigmentation. The respective stages have not been incorporated into the previously established staging system of Ballard et al. (1993) [14]. Our study furthermore complements the final stages of the Ballard system, i.e., 24 to 34, with details on morphological transitions. Most prominent are changes in external gill length and a shift in the ratio of pre- to post-vent length. Thus, our study presents a framework allowing comparison of future studies dealing with the pre-hatching stages of *Scyliorhinus*.

Supplementary Materials: The following supporting information can be downloaded at: <https://www.mdpi.com/article/10.3390/fishes7030100/s1>, Table S1: Overview of the mean and S.E.M. (mm) of selected body parameters of *S. canicula* with increasing size classes; Table S2: Overview of the mean and S.E.M. in relation to the total length (%) of selected body parameters of *S. canicula* with increasing size classes.

Author Contributions: Conceptualization, B.G.; methodology, data curation: T.R.; formal analysis: B.G. and T.R.; resources, B.G. and T.M.; writing—original draft preparation, B.G.; writing—review and editing, B.G., T.R. and T.M.; visualization, T.R., B.G. and T.M.; supervision, B.G.; project administration, B.G. All authors have read and agreed to the published version of the manuscript.

Funding: This research was funded by the Research Institute for Farm Animal Biology (FBN). The publication of this article was funded by the Open Access Fund of the FBN.

Institutional Review Board Statement: This study followed international, national, and institutional guidelines for the treatment and killing of animals and complied with Directive 2010/63/EU and the German Animal Welfare Act (§ 4(3) TierSchG). Since only unhatched sharks were used for this study, no ethics committee had to be consulted.

Data Availability Statement: All relevant data are provided within the manuscript and accompanying supplemental material.

Acknowledgments: We thank George Franz for methodical support and Katrin Tönißen and George Franz for further support within this project, as well as Lars Lewerentz from the University of Greifswald for statistical support. We further thank the aquarium team of the OZEANEUM in Stralsund, especially E. Teßmann, for taking care of the breeding group.

Conflicts of Interest: The authors have no conflicts of interest, financial or otherwise.

References

1. Bibliography Database of Living/Fossil Sharks, Rays and Chimaeras (Chondrichthyes: Elasmobranchii, Holocephali). Available online: www.shark-references.com (accessed on 12 January 2022).
2. Coolen, M.; Menuet, A.; Chassoux, D.; Compagnucci, C.; Henry, S.; Lévêque, L.; Da Silva, C.; Gavory, F.; Samain, S.; Wincker, P.; et al. The Dogfish *Scyliorhinus canicula*: A Reference in Jawed Vertebrates. *Cold Spring Harb. Protoc.* **2008**, *2008*, 3. [CrossRef] [PubMed]
3. López-Unzu, M.A.; Durán, A.C.; Rodríguez, C.; Soto-Navarrete, M.T.; Sans-Coma, V.; Fernández, B. Development of the ventricular myocardial trabeculae in *Scyliorhinus canicula* (Chondrichthyes): Evolutionary implications. *Sci. Rep.* **2020**, *10*, 14434. [CrossRef] [PubMed]
4. Aicardi, S.; Amaroli, A.; Gallus, L.; Di Blasi, D.; Ghigliotti, L.; Betti, F.; Vacchi, M.; Ferrando, S. Quantification of neurons in the olfactory bulb of the catsharks *Scyliorhinus canicula* (Linnaeus, 1758) and *Galeus melastomus* (Rafinesque, 1810). *Zoology* **2020**, *141*, 125796. [CrossRef] [PubMed]
5. Dearden, R.P.; Mansuit, R.; Cuckovic, A.; Herrel, A.; Didier, D.; Tafforeau, P.; Pradel, A. The morphology and evolution of chondrichthyan cranial muscles: A digital dissection of the elephantfish *Callorhynchus milii* and the catshark *Scyliorhinus canicula*. *J. Anat.* **2021**, *238*, 1082–1105. [CrossRef] [PubMed]

6. Bernal, D.; Sepulveda, C.; Mathieu-Costello, O.; Graham, J.B. Comparative studies of high performance swimming in sharks I. Red muscle morphometrics, vascularization and ultrastructure. *J. Exp. Biol.* **2003**, *206*, 2831–2843. [\[CrossRef\]](#)
7. Lauriano, E.; Pergolizzi, S.; Aragona, M.; Montalbano, G.; Guerrero, M.; Crupi, R.; Faggio, C.; Capillo, G. Intestinal immunity of dogfish *Scyliorhinus canicula* spiral valve: A histochemical, immunohistochemical and confocal study. *Fish Shellfish Immunol.* **2019**, *87*, 490–498. [\[CrossRef\]](#)
8. Crouch, K.; Smith, L.E.; Williams, R.; Cao, W.; Lee, M.; Jensen, A.; Dooley, H. Humoral immune response of the small-spotted catshark, *Scyliorhinus canicula*. *Fish Shellfish Immunol.* **2013**, *34*, 1158–1169. [\[CrossRef\]](#)
9. Pettinello, R.; Redmond, A.; Secombes, C.J.; Macqueen, D.J.; Dooley, H. Evolutionary history of the T cell receptor complex as revealed by small-spotted catshark (*Scyliorhinus canicula*). *Dev. Comp. Immunol.* **2017**, *74*, 125–135. [\[CrossRef\]](#)
10. Soares, K.D.A.; Carvalho, M.R. The catshark genus *Scyliorhinus* (Chondrichthyes: Carcharhiniformes: Scyliorhinidae): Taxonomy, morphology and distribution. *Zootaxa* **2019**, *4601*, 1–147. [\[CrossRef\]](#)
11. Ebert, D.A.; Dando, M. *Field Guide to Sharks, Rays & Chimaeras of Europe and the Mediterranean*; Princeton University Press: Princeton, NJ, USA, 2021; p. 383.
12. Finucci, B.; Derrick, D.; Neat, F.C.; Pacoureau, N.; Serena, F.; VanderWright, W.J. *Scyliorhinus canicula*. The IUCN Red List of Threatened Species 2021. 2021. Available online: www.iucnredlist.org/species/161307554/124478351 (accessed on 12 January 2022).
13. Compagno, L.J.V. Bullhead, mackerel and carpet sharks (*Heterodontiformes*, *Lamniformes* and *Orectolobiformes*). In *Sharks of the World. An Annotated and Illustrated Catalogue of Shark Species Known to Date*; FAO Species Catalogue for Fishery Purposes 2002; FAO: Rome, Italy, 2001; Volume 2, 269p.
14. Ballard, W.W.; Mellinger, J.; Lechenault, H. A series of normal stages for development of *Scyliorhinus canicula*, the lesser spotted dogfish (Chondrichthyes: Scyliorhinidae). *J. Exp. Zool.* **1993**, *267*, 318–336. [\[CrossRef\]](#)
15. López-Romero, F.A.; Klimpfinger, C.; Tanaka, S.; Kriwet, J. Growth trajectories of prenatal embryos of the deep-sea shark *Chlamydoselachus anguineus* (Chondrichthyes). *J. Fish Biol.* **2020**, *97*, 212–224. [\[CrossRef\]](#) [\[PubMed\]](#)
16. Grunow, B.; Kirchhoff, T.; Lange, T.; Moritz, T.; Harzsch, S. Histochemistry on vibratome sections of fish tissue: A comparison of fixation and embedding methods. *Aquat. Biol.* **2015**, *23*, 251–263. [\[CrossRef\]](#)
17. Soares, K.D.A.; Gomes, U.L.; De Carvalho, M.R. Taxonomic review of catsharks of the *Scyliorhinus haeckelii* group, with the description of a new species (Chondrichthyes: Carcharhiniformes: Scyliorhinidae). *Zootaxa* **2016**, *4066*, 501–534. [\[CrossRef\]](#) [\[PubMed\]](#)
18. Franz, G.P.; Lewerentz, L.; Grunow, B. Growth changes during the embryonic-larval-transition of pikeperch (*Sander lucioperca*). *J. Fish Biol.* **2021**, *99*, 425–436. [\[CrossRef\]](#) [\[PubMed\]](#)
19. Pedregosa, F.; Varoquaux, G.; Gramfort, A.; Michel, V.; Thirion, B.; Grisel, O.; Blondel, M.; Prettenhofer, P.; Weiss, R.; Dubourg, V.; et al. Scikit-learn: Machine Learning in Python. *J. Mach. Learn. Res.* **2011**, *12*, 2825–2830.
20. Hunter, J.D. Matplotlib: A 2D graphics environment. *Comput. Sci. Eng.* **2007**, *9*, 90–95. [\[CrossRef\]](#)
21. Waskom, M.; Botvinnik, O.; Ostblom, J.; Gelbart, M.; Lukauskas, S.; Hobson, P.; Gempert, D.C.; Augspurger, T.; Yaroslav, H.; Cole, J.B.; et al. *Mwaskom/Seaborn: V0.10.1 (April 2020)*; Version v0.10.1; Zenodo: Geneva, Switzerland, 2020. [\[CrossRef\]](#)
22. Didier, D.A.; LeClair, E.E.; Vanbuskirk, D.R. Embryonic staging and external features of development of the Chimaeroid fish, *Callorhynchus milii* (Holocephali, Callorhynchidae). *J. Morphol.* **1998**, *236*, 25–47. [\[CrossRef\]](#)
23. Maxwell, E.E.; Fröbisch, N.B.; Heppleston, A.C. Variability and Conservation in Late Chondrichthyan Development: Ontogeny of the Winter Skate (*Leucoraja ocellata*). *Anat. Rec.* **2008**, *291*, 1079–1087. [\[CrossRef\]](#)
24. Rodda, K.R.; Seymour, R.S. Functional morphology of embryonic development in the Port Jackson shark *Heterodontus portusjacksoni* (Meyer). *J. Fish Biol.* **2008**, *72*, 961–984. [\[CrossRef\]](#)
25. Musa, S.M.; Ripley, D.M.; Moritz, T.; Shiels, H.A. Ocean warming and hypoxia affect embryonic growth, fitness and survival of small-spotted catsharks, *Scyliorhinus canicula*. *J. Fish Biol.* **2020**, *97*, 257–264. [\[CrossRef\]](#)
26. Tanaka, S.; Shiobara, Y.; Hioki, S.; Abe, H.; Nishi, G.; Yano, K.; Suzuki, K. The Reproductive Biology of the Frilled Shark, *Chlamydoselachus anguineus*, from Suruga Bay, Japan. *Jpn. J. Ichthyol.* **1990**, *37*, 273–291.
27. Onimaru, K.; Motone, F.; Kiyatake, I.; Nishida, K.; Kuraku, S. A staging table for the embryonic development of the brownbanded bamboo shark (*Chiloscyllium punctatum*). *Dev. Dyn.* **2018**, *247*, 712–723. [\[CrossRef\]](#) [\[PubMed\]](#)
28. Hook, S.A.; McMurray, C.; Ripley, D.; Allen, N.; Moritz, T.; Grunow, B.; Shiels, H.A. Recognition software successfully aids the identification of individual small-spotted catsharks *Scyliorhinus canicula* during their first year of life. *J. Fish Biol.* **2019**, *95*, 1465–1470. [\[CrossRef\]](#)
29. Crooks, N.; Babey, L.; Haddon, W.J.; Love, A.C.; Waring, C.P. Sexual Dimorphisms in the Dermal Denticles of the Lesser-Spotted Catshark, *Scyliorhinus canicula* (Linnaeus, 1758). *PLoS ONE* **2013**, *8*, e76887. [\[CrossRef\]](#) [\[PubMed\]](#)
30. Ford, E. A Contribution to Our Knowledge of the Life-Histories of the Dogfishes Landed at Plymouth. *J. Mar. Biol. Assoc.* **1921**, *12*, 468–505. [\[CrossRef\]](#)
31. Filiz, H.; Taskavak, E. Sexual dimorphism in the head, mouth, and body morphology of the small spotted catshark, *Scyliorhinus canicula* (Linnaeus, 1758) (Chondrichthyes: Scyliorhinidae) from Turkey. *Acta Adriat.* **2006**, *47*, 37–47.